Mucosal Immunology 18 (2025) 76–89

Contents lists available at ScienceDirect

Mucosal Immunology

journal homepage: www.elsevier.com/mi

Combined plasma protein and memory T cell profiling discern IBD-patient-immunotypes related to intestinal disease and treatment outcomes

Maud Heredia [a,1], Mohammed Charrout [b,1], Renz C.W. Klomberg [c,1], Martine A. Aardoom [c], Maria M.E. Jongsma [c], Polychronis Kemos [d], Danielle H. Hulleman-van Haaften [a], Bastiaan Tuk [a], Lisette A. van Berkel [a], Brenda Bley Folly [a], Beatriz Calado [a], Sandrine Nugteren [a,e], Ytje Simons-Oosterhuis [a], Michail Doukas [e], Mathijs A. Sanders [f], Gregory van Beek [f], Frank M. Ruemmele [h], Nicholas M. Croft [d], Ahmed Mahfouz [b,g], Marcel J.T. Reinders [b], Johanna C. Escher [c], Lissy de Ridder [c], Janneke N. Samsom [a,*]

[a] Laboratory of Pediatrics, Division Gastroenterology and Nutrition, Erasmus University Medical Center, Rotterdam, The Netherlands
[b] Delft Bioinformatics Lab, Delft University of Technology, Delft, The Netherlands
[c] Department of Pediatric Gastroenterology, Erasmus University Medical Center-Sophia Children's Hospital, Rotterdam, The Netherlands
[d] Centre for Immunobiology, Blizard Institute, Queen Mary University of London, London, UK
[e] Department of Pathology, Erasmus University Medical Center, Rotterdam, The Netherlands
[f] Department of Hematology, Erasmus MC Cancer Institute, Erasmus University Medical Center, Rotterdam, The Netherlands
[g] Department of Human Genetics, Leiden University Medical Center, Leiden, The Netherlands
[h] Department of Pediatric Gastroenterology, Necker-Enfants Malades University Hospital, Institut Imagine, AP-HP, Université Paris Cité, Paris, France

ARTICLE INFO

Keywords:
Proteomics
Memory CD4$^+$ T cells
ex-Th17
Neutrophils

ABSTRACT

Inflammatory bowel disease (IBD) chronicity results from memory T helper cell (Tmem) reactivation. Identifying patient-specific immunotypes is crucial for tailored treatment. We conducted a comprehensive study integrating circulating immune proteins and circulating Tmem, with intestinal tissue histology and mRNA analysis, in therapy-naïve pediatric IBD (Crohn's disease, CD: $n = 62$; ulcerative colitis, UC: $n = 20$; age-matched controls $n = 43$), and after 10–12 weeks' induction therapy. At diagnosis, plasma protein profiles unveiled two UC and three CD clusters with distinct disease courses. UC patients displayed unchanged circulating Tmem, while CD exhibited increased frequencies of gut-homing ex-Th17, known for high IFN-γ production. UC#2 had elevated Th17/neutrophil-pathway-related proteins and severe disease, with higher endoscopic and histological damage and Th17/neutrophil infiltration. Although both UC#1 and UC#2 responded to therapy, UC#2 required earlier immunomodulation. CD#3 had lower plasma protein concentrations, especially IFN-γ pathway proteins, fewer gut-homing ex-Th17 and clinically milder disease, confirmed by intestinal gene expression. CD#1 and CD#2 had comparably high Th1-related immune profiles, but CD#1 exhibited higher concentrations of proteins previously associated with poorer prognosis. Both CD clusters responded to induction therapy, with similar one-year outcomes. This study highlights feasibility of discriminating patient-specific immunotypes in IBD, advancing our understanding of immune pathogenesis, needed for tailored treatment strategies.

Introduction

Inflammatory bowel disease (IBD), a chronic inflammation of the gastrointestinal tract, has two clinical subtypes: Crohn's disease (CD) and ulcerative colitis (UC). In genetically susceptible individuals, loss of intestinal barrier integrity and increased interaction of the intestinal microbiota with immune cells lead to aberrant inflammatory T helper cell (Th) responses.[1,2] Immunomodulators, immunosuppressants, and biologics including anti-TNFα, anti-IL-12/23p40, anti-α4β7 suppress

* Corresponding author at: P.O. Box 2040, 3000 CA Rotterdam, The Netherlands.
E-mail address: j.samsom@erasmusmc.nl (J.N. Samsom).
[1] Authors share first authorship.

https://doi.org/10.1016/j.mucimm.2024.09.004
Received 8 April 2024; Accepted 21 September 2024
Available online 26 September 2024

Non-standard abbreviations

5-ASA	5-aminosalicylates
ADA	adenosine deaminase
CCL	C–C chemokine ligand
CCR	C–C chemokine receptor
CDCP1	CUB domain-containing protein 1
CRP	C-reactive protein
CXCL	C-X-C chemokine ligand
DEG	differentially expressed genes
DNER	Delta and Notch-like epidermal growth factor-related receptor
EEN	exclusive enteral nutrition
ESR	erythrocyte sedimentation rate
FGF	fibroblast growth factor
Flt3L	Fms-like tyrosine kinase 3 ligand
GHAS	global histological disease activity score
HC	healthy controls
HGF	hepatocyte growth factor
HLADR	human leukocyte antigen-DR
IBDneg	IBD-negative
IBD-U	IBD-unclassified
IFN	interferon
IL	interleukin
MDR	multidrug resistance protein
MHC	major histocompatibility complex
MMP	matrix metalloproteinase
NPX	normalized protein expression
OSM	oncostatin M
PD-L1	programmed cell death ligand 1
PUCAI	pediatric UCAI
SCF	stem cell factor
SES	simple endoscopy score
Th	T helper
Tmem	memory T helper cell
TNF	tumor necrosis factor
TNFSF	TNF superfamily
TRANCE	TNF-related activation-induced cytokine
UCEIS	UC endoscopic index of severity
VEGFA	vascular endothelial growth factor A
wPCDAI	weighted pediatric CDAI

induction, survival, or recruitment of T helper cells. Unfortunately, some patients do not respond well and become refractory. Thus, novel tailored treatment strategies are needed to target each patient's underlying immune disease. However, knowledge of the subtypes of Th responses that drive disease in individual patients is very limited.

The chronicity of IBD is driven by reactivation of cytokine-secreting memory Th (Tmem) in the lamina propria. In the mucosa, IL-17A production increases in both CD and UC[3]. Increased IFN-γ and TNF-α are more predominant in CD, while increased IL-5 and IL-13 are detected in some UC patients.[4,5] Various subpopulations of Tmem may produce these cytokines. Indeed, Th17 cells increase in the mucosa in both CD and UC, Th1 cells increase in CD, and Th2 cells increase in UC.[6,7] However, additional populations with a mixed Th17 and Th1 phenotype have recently been identified in CD.[8,9] Described as ex-Th17 cells that acquire features of Th1 cells upon inflammation, these Th17/Th1, Th17.1, and Th1* cells are pathogenic in multiple autoimmune and inflammatory disorders.[10] Their contribution to CD and UC are unclear as Tmem are not routinely enumerated.

In the intestine, Th-derived cytokines skew different patterns of immune activation, e.g., IFN-γ upregulates MHC-II and stimulates phagocytosis and killing by phagocytes, while IL-17A reinforces intestinal barrier integrity, drives release of epithelial antimicrobial peptides by epithelial cells, and recruits neutrophils.[11–15] Upon sensing bacterial translocation or tissue damage in combination with local Th-derived cytokines, epithelial cells and myofibroblasts produce defined mixtures of chemokines to selectively recruit the circulating Th needed for host defense to damaged tissue. For example, CXCL9, CXCL10, and CXCL11—IFN-γ-induced chemokine ligands for CXCR3 on circulating Th1 cells—are increased in CD and UC lesions.[16] Analogously, CCL20 and its receptor CCR6, expressed by Th17 cells, are increased in the mucosa in IBD.[17] Although produced in the intestine, increased concentrations of these cytokines can be detected in the circulation. As different Th-derived cytokines and tissue damage elicit tailored chemokine and cytokine cascades, peripheral blood immune profiling could capture the ongoing immune response in individual patients.

Recent highly sensitive, specific proximity-based assays have enabled immune protein profiling studies. For example, plasma immune protein concentrations distinguished patients with UC and irritable bowel syndrome[18] and immune profiles predict disease complications in IBD.[19–21] Moreover, we recently established that pretreatment serum immune protein profiles could predict clinical responses to conventional and first-line infliximab treatment at one year in pediatric CD.[22]

Here, we advance these promising observations in a comprehensive longitudinal analysis that relates plasma immune protein profiles to circulating Tmem responses and intestinal immune disease in clinically well-characterized therapy-naïve pediatric patients with CD or UC.

Results

Cohort description

After Olink® quality control, the final baseline population included 62 CD patients (30 in PIBD-SETQuality, 22 in TISKIDS, 10 in both studies), 20 UC patients (PIBD-SETQuality), 30 pediatric healthy controls (HC) without intestinal complaints, and 13 IBD-negative (IBDneg) patients **(**Table S2**)**. At 10–12 weeks, 56 CD and 13 UC patients passed Olink® quality control. Baseline characteristics for all patients are shown in Table S3. HC were slightly younger (median, 12.3 years; IQR, 10.4–15.1) than the median age at diagnosis of IBD children (14.6 years; IQR, 12.1–16.1; $P = 0.02$). Age was not associated with protein profiles in HC.

CD and UC patients exhibit shared and distinct protein and cellular immune profiles in blood at diagnosis

At diagnosis, plasma immune protein profiles of CD and UC patients exhibited shared features, but also differed ($P < 0.05$ $|Log2FC|>0.5$) to HC (Fig. 1**A, S1A**). Profiles of IBDneg patients and age-matched HC were similar (Fig. S1**B, S2A**); therefore grouped and denoted as HC. The concentrations of 29 proteins varied between CD and HC, 22 differed between UC and HC, and 5 differed between UC and CD (Fig. S2**B-D**). As expected, increased concentrations of the Th1 cytokine IFN-γ were strongly associated with CD, whereas Th17-associated IL-17A was increased in UC (Fig. 1**B**). Th2-related IL-5 and IL-13—sometimes associated with UC—were similar in UC and HC (Fig. 1**B**). No differences between UC and CD were associated with disease activity (Table S3). Seventeen proteins were increased in CD and UC vs. HC; the top 5 shared proteins with highest fold changes were CXCL9, IL-6, OSM, IL-8/CXCL8, and IL-17A (Fig. 1**B, S2B-C**). While IL-17A and IL-8 correlated positively with endoscopic intestinal inflammation (UCEIS and SESCD), CXCL9, IL-6, and OSM correlated positively with blood platelets, erythrocyte sedimentation rate (ESR), and C-reactive protein (CRP) and correlated

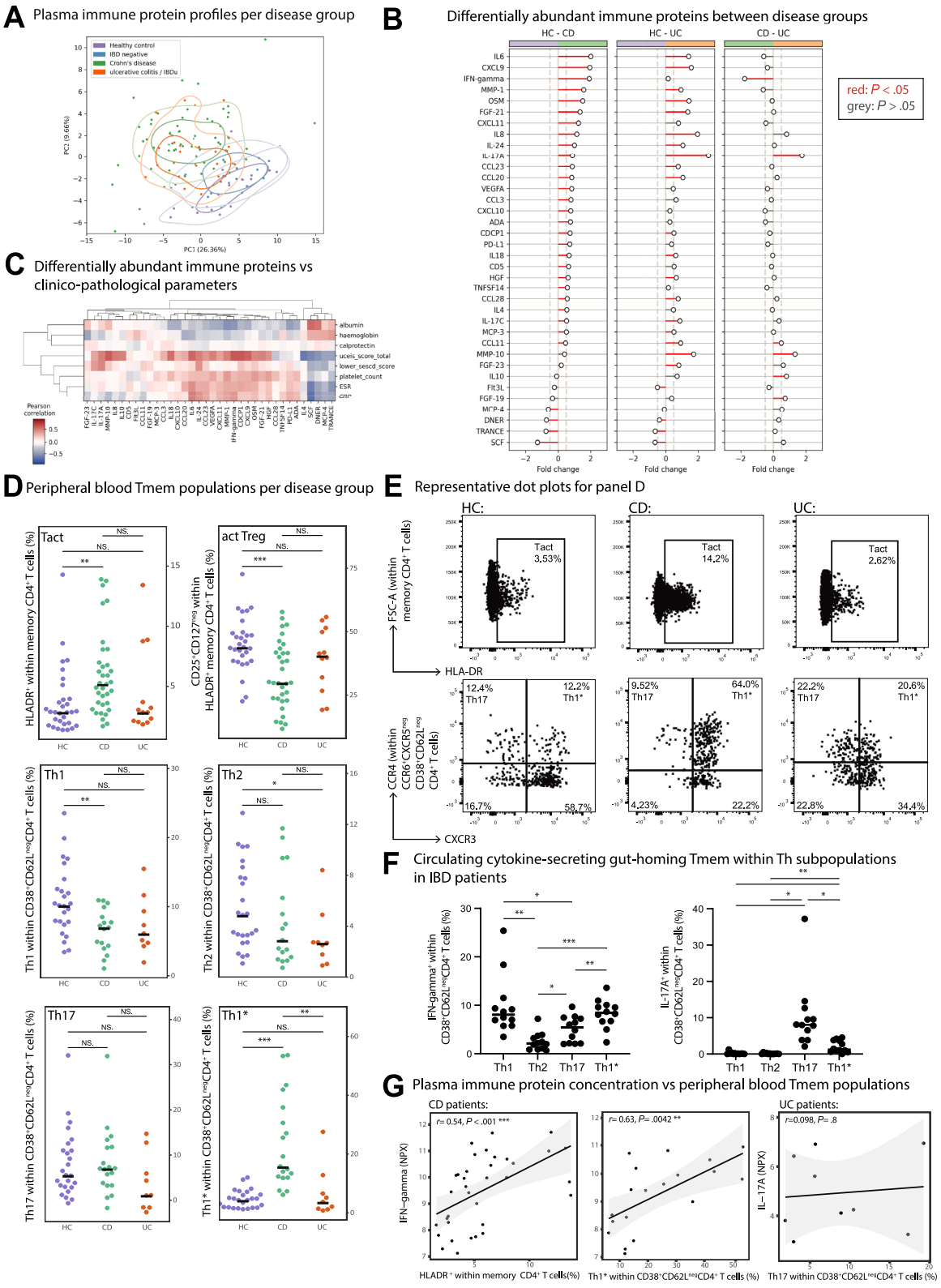

Fig. 1. IBD-related plasma immune protein concentrations at diagnosis are associated with clinicopathological parameters, peripheral blood Tmem populations and identify unique CD and UC signatures. A: Principal component analysis of all plasma immune protein concentrations per disease. B: Fold change in median concentrations of the 36 differentially abundant proteins (CD vs. HC, UC vs. HC, and UC vs. CD). C: Correlation matrix of differential proteins and clinicopathological parameters; Pearson's correlation coefficient. D: Frequencies of peripheral blood Tmem subpopulations per disease group. Bar indicates median frequencies. Gating strategies and calculations of frequencies are explained in Fig. S3B-C; Student *t* test. E: Representative dot plots of Tact (HLADR^{+} within CD45RA^{neg}CD4^{+}CD8^{neg}, see Fig. S3B for gating strategy), Th17 (CXCR3^{neg}CCR4^{+}) and Th1* (CXCR3^{+}CCR4^{+}) within CCR6^{+}CXCR5^{neg}CD38^{+}CD62L^{neg}CD4^{+}CD3^{+}Live/Dead^{neg} (see Fig. S3C for gating strategy) in CD, UC and HC. F: IFN-γ and IL-17A-secreting gut-homing Tmem frequencies in Th subpopulations after restimulation of peripheral blood of therapy-naïve IBD patients. Repeated measures one-way ANOVA, Bonferroni's multiple comparisons test. G: Correlation analysis of plasma IFN-γ and IL-17A (NPX) and circulating Tmem frequencies; Pearson's correlation coefficient (*r*). NS: not significant, *: $P < 0.05$, **: $P < 0.01$, ***: $P < 0.001$.

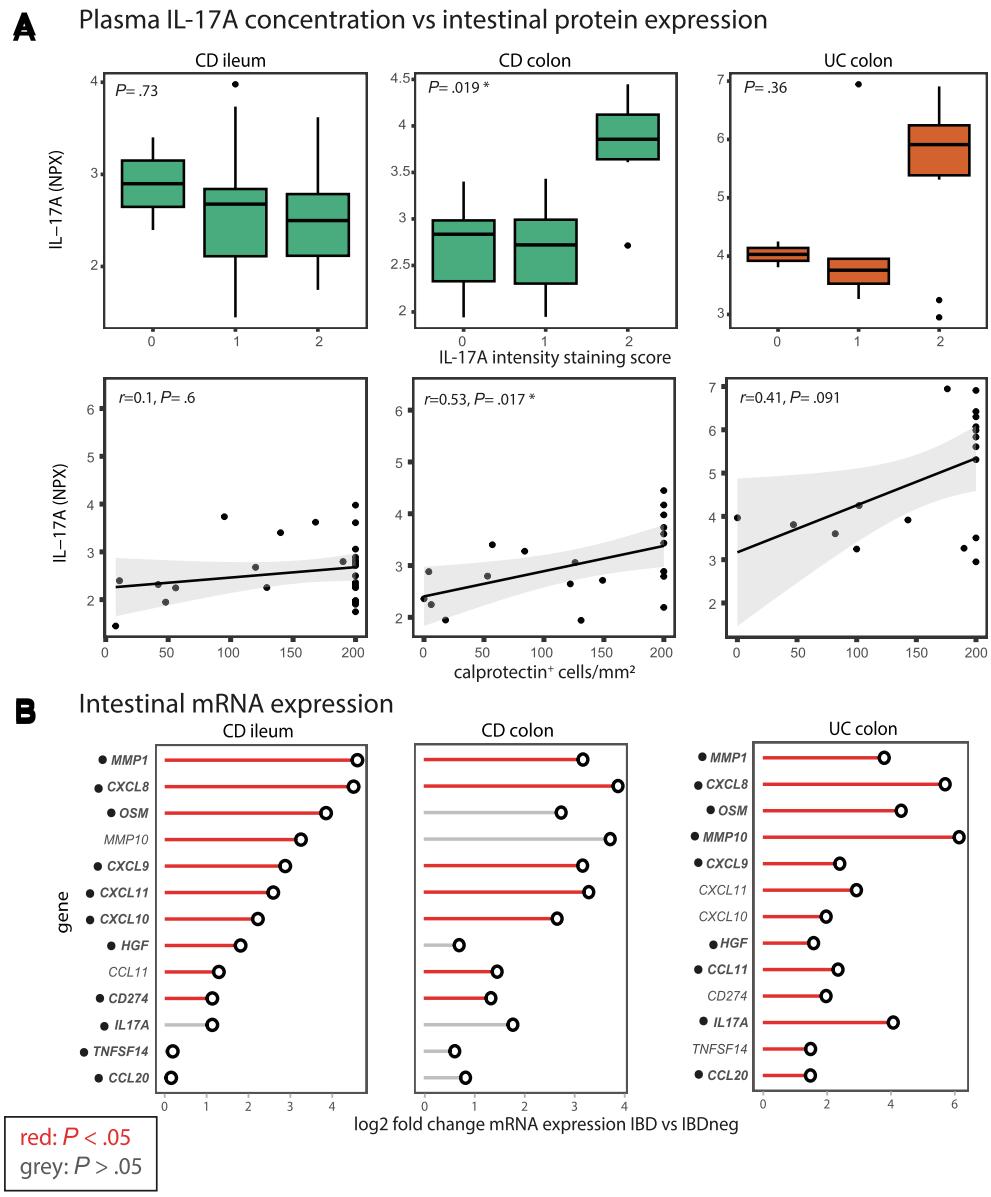

Fig. 2. IBD-related plasma immune protein concentrations at diagnosis are associated with intestinal protein and mRNA expression. A: Plasma IL-17A (NPX) versus IL-17A intestinal immunohistochemical score and calprotectin-positive cells/mm^2 in CD and UC ileum and colon. Box plots: Kruskall-Wallis test; correlation plots: Spearman's correlation coefficient (*r*). B: Log2 fold changes in differentially expressed genes (DEGs; RNA sequencing of biopsies) matching differential plasma proteins. Bold font indicates DEGs that match significantly differential proteins in CD and UC vs. HC.

negatively with albumin and hemoglobin (Fig. 1**C**), in line with our previous study.[22] In contrast, SCF, TRANCE, DNER, MCP-4, and Flt3L (which were lower in IBD than HC) negatively correlated with endoscopic score, platelet count, ESR, and CRP and positively correlated with albumin and hemoglobin, suggesting higher concentrations of these proteins are associated with better clinical status (Fig. 1**C**).

In line with the discriminative immune protein profiles, Tmem frequencies in peripheral blood at diagnosis were heterogeneous and significantly differed between CD, UC, and HC (Fig. 1**D**). A selective increase in HLADR$^+$ Tmem frequencies, defined as activated T cells (Tact), was detected in CD vs. UC and HC (Fig. 1**D-E**). Within this Tact population, the Treg phenotype (CD127^{lo}CD25^{hi} cells, or actTreg) was only decreased in CD, indicating ongoing immune activation. In agreement, frequencies of CD25$^+$Foxp3$^+$ within Tact were also decreased in CD (Fig. S3**A-B**). To discriminate Tmem with gut-homing capacity, we monitored CD38$^+$CD62L^{neg} Tmem (mean ~ 2 % of total CD4$^+$ T cells) that are highly enriched in α4β7$^+$ cells[23] (gating strategy in Fig. S3**C**). Unexpectedly, despite the high IFN-γ concentrations in CD, Th1 frequencies within gut-homing CD38$^+$CD62L^{neg} Tmem were decreased in CD and UC vs. HC (Fig. 1**D**). Deeper analysis revealed increased frequencies of Th1* cells (CXCR3$^+$CCR4$^+$ CCR6$^+$CXCR5^{neg}) in gut-homing CD38$^+$CD62L^{neg} Tmem in CD vs. HC and UC (Fig. 1**D-E**). Th1* cells, a subset of ex-Th17 cells that have shifted initial differentiation to Th1-like cells, produce high concentrations of IFN-γ and are pathogenic drivers in several inflammatory disorders.[10] In comparison, the frequencies of Th17 (CXCR3^{neg}CCR4$^+$CCR6$^+$CXCR5^{neg}) within gut-homing CD38$^+$CD62L^{neg} Tmem were unchanged while Th2 frequencies were slightly decreased in UC vs. HC.

IBD plasma immune protein concentrations at diagnosis relate to circulating Tmem frequencies and intestinal protein and gene expression

To assess the intracellular cytokine production of the different Th subpopulations identified in circulating gut-homing Tmem, we re-

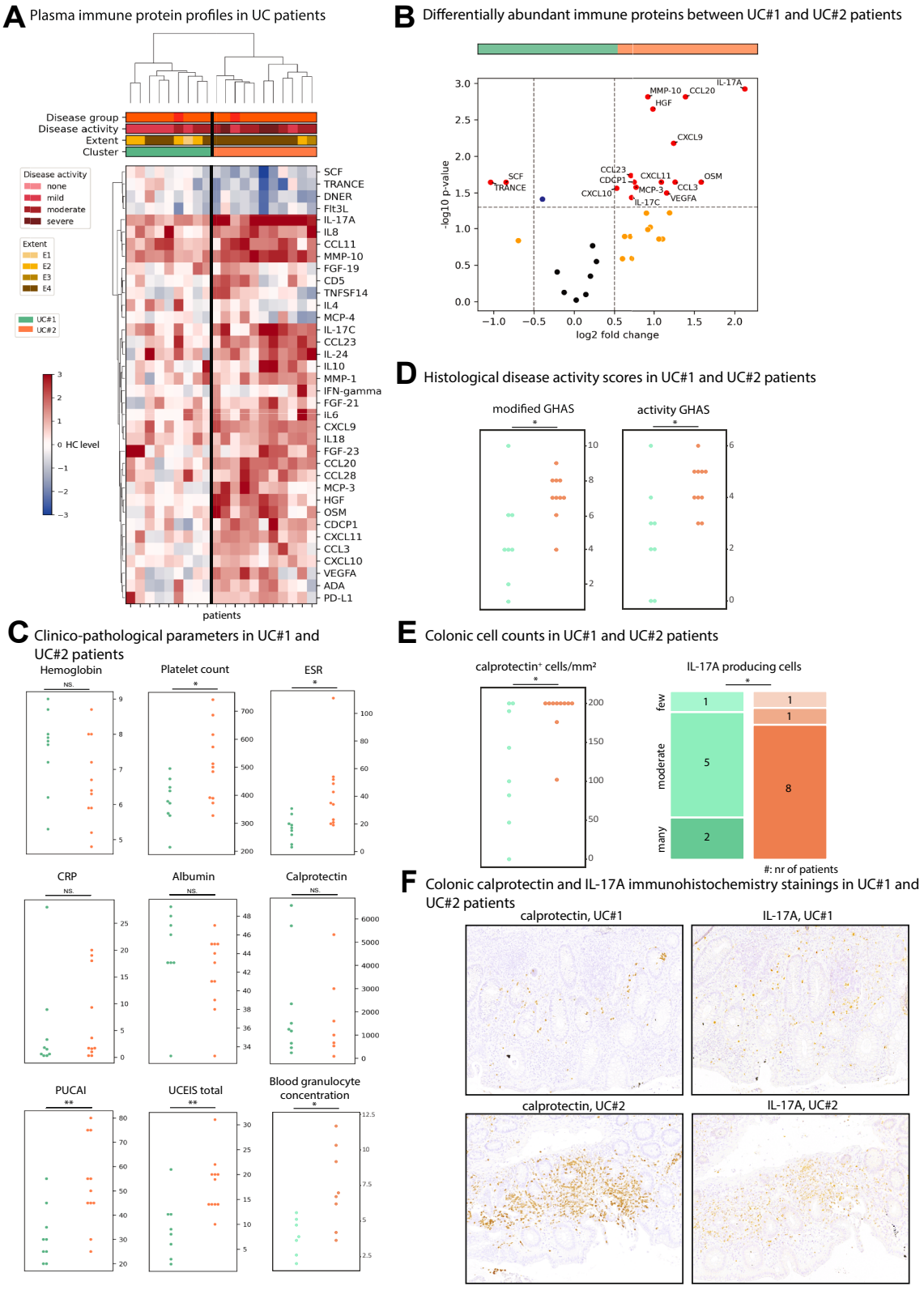

Fig. 3. Hierarchical clustering of plasma immune protein profiles at diagnosis identifies two UC clusters, with UC#2 having increased clinical and endoscopic disease severity and an intestinal Th17/neutrophil signature. A: Hierarchical clustering with Ward linkage of the 36 differentially abundant proteins in UC. Concentrations are z-scores of fold change vs. HC. Two clusters are identified: UC#1 and UC#2. Top bars represent PUCAI and Paris classification. B: Volcano plot of differential proteins between clusters. C: Clinicopathological parameters; Student *t* test. D: Histological disease activity scores; Wilcoxon-Mann-Whitney test. E: Calprotectin-positive cells/mm^2 and immunohistochemical scoring of IL-17A-producing cells in colonic biopsies; Wilcoxon-Mann-Whitney test (right), Fisher's exact test (left). F: Representative immunohistochemical co-localization of calprotectin (left) and IL-17A (right)-positive cells in serial sections of colonic biopsies. NS: not significant, *: $P < 0.05$, **: $P < 0.01$.

stimulated peripheral blood mononuclear cells (PBMC) from a limited number of therapy-naïve CD and UC patients for whom we had sufficient numbers of cells. These data confirm that both Th1 and Th1* are the main producers of IFN-γ, whereas Th17 and Th1* are the main producers of IL-17A in IBD patients (Fig. 1**F**). The increased Tact frequencies in CD correlated with high plasma IFN-γ (Fig. 1**G**). Crucially, Th1* frequencies within gut-homing $CD38^{+}CD62L^{neg}$ Tmem also significantly correlated with high plasma IFN-γ in CD. In agreement, CD patients with high plasma IFN-γ had higher frequencies of IFN-γ secreting gut-homing Tmem (Fig. S3**E**). As anticipated based on the minor changes in Tmem frequencies in UC, no correlations were observed between plasma IL-17A (or CCL20, **data not shown**) and circulating Tmem frequencies. In particular, IL-17A did not correlate with Th17 frequencies or frequencies of IL-17 secreting cells within gut-homing $CD38^{+}CD62L^{neg}$ Tmem (Fig. 1**G,** Fig. S3**E**). In healthy intestine, Th17 responses are continuously present and actively maintain homeostasis.[24] Therefore, we hypothesized that the increased plasma IL-17A in CD and UC derive from expansion of local intestinal Th17 Tmem and, in contrast to IFN-γ, does not require recruitment of circulating Th17 Tmem. To explore this, we related immunohistochemical IL-17A staining and neutrophil infiltration in biopsies to plasma IL-17A. In CD, increased plasma IL-17A was significantly associated with increased IL-17A and neutrophil abundance (calprotectin-positive cells/mm^2) in colonic lesions but not terminal ileum (Fig. 2**A**). In UC, these associations were more heterogeneous and non-significant (Fig. 2**A**). Thus, plasma IL-17A is significantly related to local colonic Th17 responses and subsequent neutrophil-driven disease.

In further confirmation that increases in plasma proteins correlate with intestinal tissue immune responses, 13/36 differentially abundant plasma proteins were differentially expressed at the mRNA level in ileal or colonic lamina propria in IBD vs. IBDneg (Fig. 2**B**). In CD, the strong plasma protein Th1 signature was detectable in both ileal and colonic biopsies (*CXCL9, CXCL10, CXCL11, PD-L1/CD274*). A strong Th17 signature (*IL-17A, CCL20*) was detected in UC biopsies.

Plasma IFN-γ and IL-17A concentrations relate to histological disease severity

To assess whether plasma protein concentration responses reflect intestinal damage, histological disease was quantified using the modified GHAS (tissue infiltration of mononuclear and polymorphonuclear cells, tissue damage). The activity GHAS sub-score assesses active disease based on neutrophil infiltration, epithelial damage, and erosions or ulcers. As a control, we first analyzed intestinal expression of IL-1β, a key pathogenic cytokine that is strongly upregulated in CD and UC.[25,26] Intestinal IL-1β-positive cell counts per mm^2 in ileum (CD) and colon (CD and UC) significantly correlated with histological disease activity in both CD and UC, demonstrating that increased immune activation can reliably be detected and relates to histological disease severity in both ileal and colonic biopsies (Fig. S4**A-B**).

In CD, high IL-17A plasma correlated with the severity of histological disease (modified and activity GHAS) in the colon but not ileum (Fig. S4**A**). In UC, these correlations were heterogeneous and non-significant (Fig. S4**B**). Though not associated with histological ileal or colonic disease severity in CD, plasma IFN-γ was significantly associated with the modified and activity GHAS in UC (Fig. S4**A-B**). These counterintuitive results suggest that increased plasma Th17- and Th1-related profiles can be detected in the most severe CD and UC patients, respectively.

These data establish that plasma immune protein profiles at diagnosis discriminate IBD from HC. Overall, the profiles of CD and UC overlap, but exhibit key IFN-γ and IL-17A pathway signatures, respectively. In CD, plasma IFN-γ signatures correlate with circulating Tmem frequencies; in UC, circulating Tmem frequencies are not elevated. Crucially, the plasma immune responses are associated with intestinal histological disease severity, pattern of immune infiltration and mRNA expression.

Hierarchical clustering of plasma immune protein profiles at diagnosis identifies two clusters of UC patients with differing clinical and endoscopic disease severity

Hierarchical clustering identified two UC clusters with lower (green, UC#1) or higher (orange, UC#2) concentrations of the 36 plasma IBD-associated inflammatory proteins (Fig. 3**A**). Age was not associated with protein profiles in UC (Table S4). UC#1 and UC#2 shared four increased (IL-17A, IL-8, CCL11, MMP-10) and four reduced proteins (SCF, TRANCE, DNER, Flt3L). Sixteen proteins differed ($P < 0.05$, $|\log2FC| > 0.5$) between UC#1 and UC#2 (Fig. 3**B**). UC#2 patients had an increased Th1-related signature (CXCL9, CXCL10, CXCL11, CDCP1), increased Th17/neutrophil-related signature (IL-17A, CCL20, CCL3, IL-17C), and decreased TRANCE and SCF vs. UC#1 (Fig. 3**B, S5A**). Ten of 11 UC#2 patients had extensive disease (E3-E4) vs. 4/9 UC#1 patients ($P = 0.08$). Endoscopic disease scores were significantly higher in UC#2 (19 vs. 8.5, $P = 0.007$), suggesting larger intestinal tissue involvement in UC#2 (Table S4). Moreover, UC#2 had significantly higher platelet counts, ESR, and clinical disease activity scores, reflecting more severe clinical and intestinal disease (Fig. 3**C,** Table S4), and higher circulating granulocytes (Fig. 3**C),** reflecting increased neutrophil recruitment. Peripheral blood Tmem frequencies were not different between UC#2 and UC#1 (Fig. S5**B**).

UC#2 has increased microscopic Th17/neutrophilic intestinal disease vs. UC#1

Beyond the difference in affected surface area, UC#2 lesional colonic biopsies exhibited increased histological damage (modified GHAS, activity GHAS) and neutrophil infiltration (calprotectin-positive cells/mm^2) vs. UC#1 (Fig. 3**D-E,** Table S4). Crucially, IL-17A-producing cells were also increased in colonic biopsies—and co-localized with neutrophils—in UC#2 (Fig. 3**E-F**). IL-1β-positive cell numbers were similar (Fig. S5**C**) and RNA-sequencing did not uncover any differences in Th17 or Th1 signature genes between UC#1 and UC#2 colonic biopsies (Fig. S5**D**).

Thus, the 36 plasma proteins can discriminate UC patients with more extensive and clinically more severe disease. UC#2 lesional biopsies exhibited increased histologic disease and Th17/neutrophilic infiltration and a striking plasma Th1-related signature.

Hierarchical clustering of plasma immune protein profiles at diagnosis identifies three clusters of CD patients with different clinicopathological features

Similar hierarchical clustering at diagnosis identified three groups of CD patients: CD#1 with highly increased concentrations of inflammatory proteins (orange), CD#2 with intermediate concentrations (blue), and CD#3 with lower concentrations (green; Fig. 4**A**). Age was not associated with protein profiles in CD (Table S5). All clusters had lower abundances of a network of proteins (IL-10, FGF-19, Flt3L, DNER, SCF, MCP-4, TRANCE) with mixed functions, including immune regulation and monocyte chemotaxis. CD#3 more strongly differed to CD#1 (25 significantly different proteins) than CD#2 (14 proteins; Fig. 4**B**). Proportions of patients with perianal disease and distribution of macroscopic inflammation were comparable between the three clusters (Table S5) but, in line with the overall lower abundance of circulating inflammatory proteins, CD#3 had significantly lower platelet counts, ESR, CRP, and wPCDAI scores and higher albumin than CD#1 and CD#2, inferring less severe disease (Fig. 4**C**). Endoscopic disease activity and peripheral blood granulocyte concentrations did not differ between clusters (Fig. 4**C**). In agreement with less severe disease, CD#3 also had significantly lower IFN-γ than CD#1 and CD#2 (Fig. S6**A,** Fig. 4**B**). Despite having relatively mild disease, a small subgroup of five CD#3

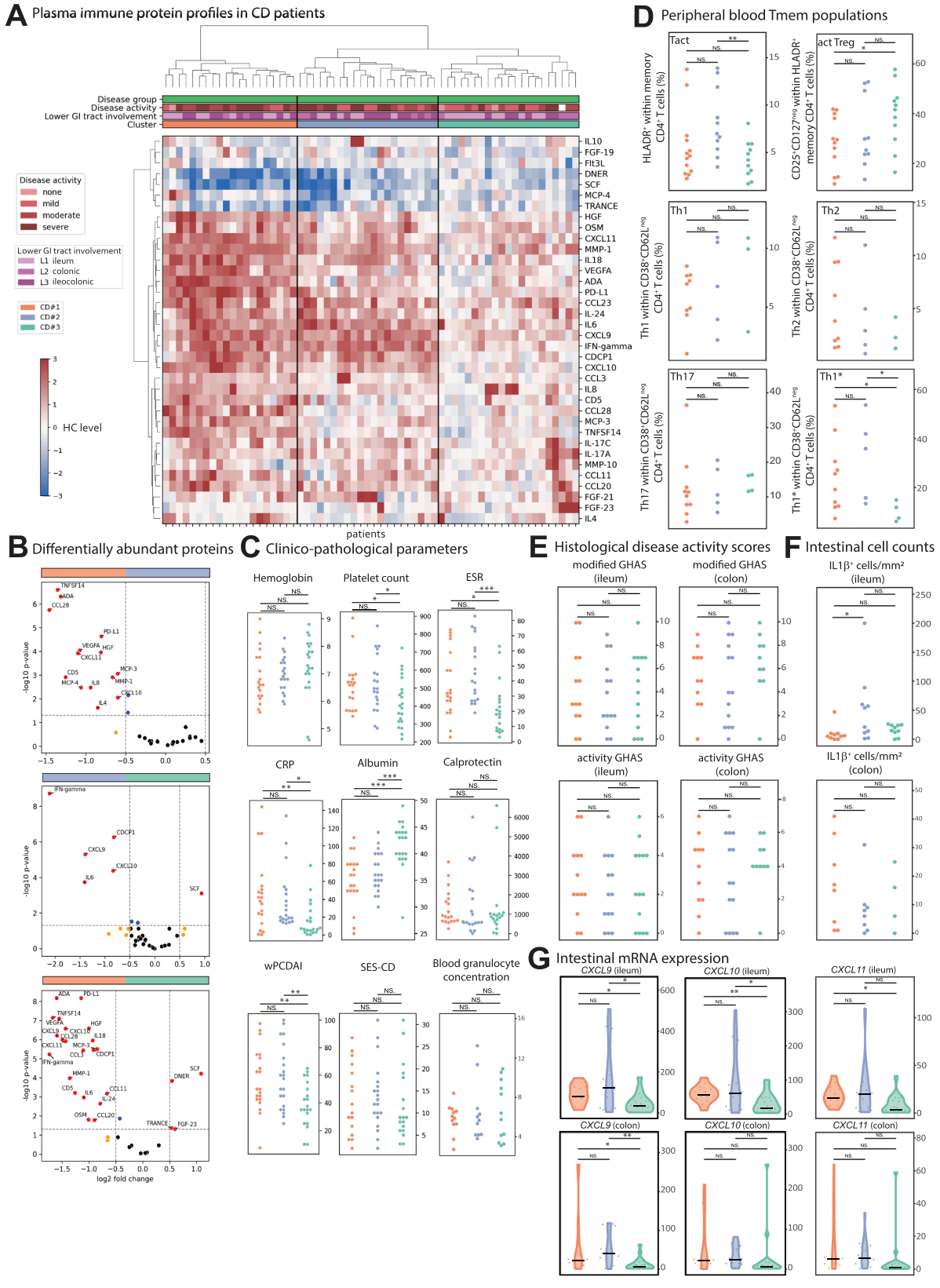

Fig. 4. Hierarchical clustering of plasma immune protein profiles identifies three CD clusters, with CD#3 having reduced clinical disease severity and an inflammatory ex-Th17/IFN-γ signature in blood and tissue. A: Hierarchical clustering with Ward linkage of the 36 differentially abundant proteins in CD. Concentrations are z-scores of fold changes vs. HC. Three clusters are differentiated: CD#1, CD#2, and CD#3. Top bars represent wPCDAI and Paris classification. B: Volcano plots of differential proteins between clusters. C: Clinicopathological parameters; Student *t* test. D: Peripheral blood Tmem frequencies; Student *t* test. E: Histological disease activity scores in ilial and colonic biopsies; Wilcoxon-Mann-Whitney test. F: IL-1β-positive cells in ileal and colonic biopsies; Wilcoxon-Mann-Whitney test. G: Differentially expressed genes in paired biopsies matching differential plasma proteins. NS: not significant, *: $P < 0.05$, **: $P < 0.01$, ***: $P < 0.001$.

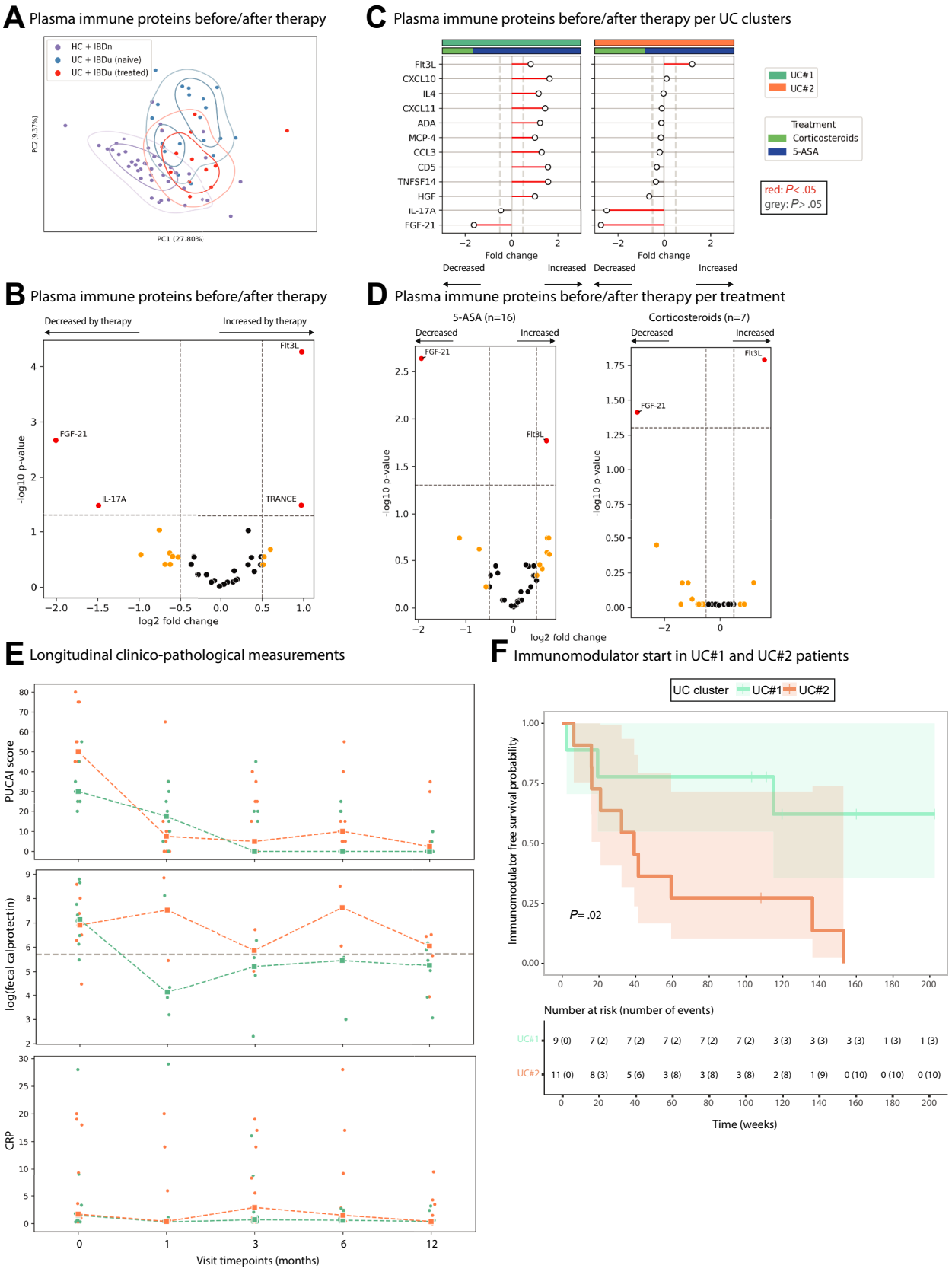

Fig. 5. Plasma protein concentrations normalize in both UC clusters in response to therapy, with earlier initiation of immunomodulators in UC#2. A: Principal component analysis of all protein concentrations at t = 0 and t = 10–12 weeks (treated). B: Volcano plot of the 36 differential proteins at t = 10–12 weeks vs. t = 0. C: Fold changes in differential proteins in UC#1 and UC#2 at t = 10–12 weeks vs. t = 0. D: Volcano plot of differential proteins at t = 10–12 weeks vs. t = 0 stratified by therapy. E: Longitudinal analysis of PUCAI, fecal calprotectin, and C-reactive protein per cluster. Dashed line indicates 300 mg/L fecal calprotectin. F: Kaplan-Meier curves of immunomodulatory-free survival; log-rank test.

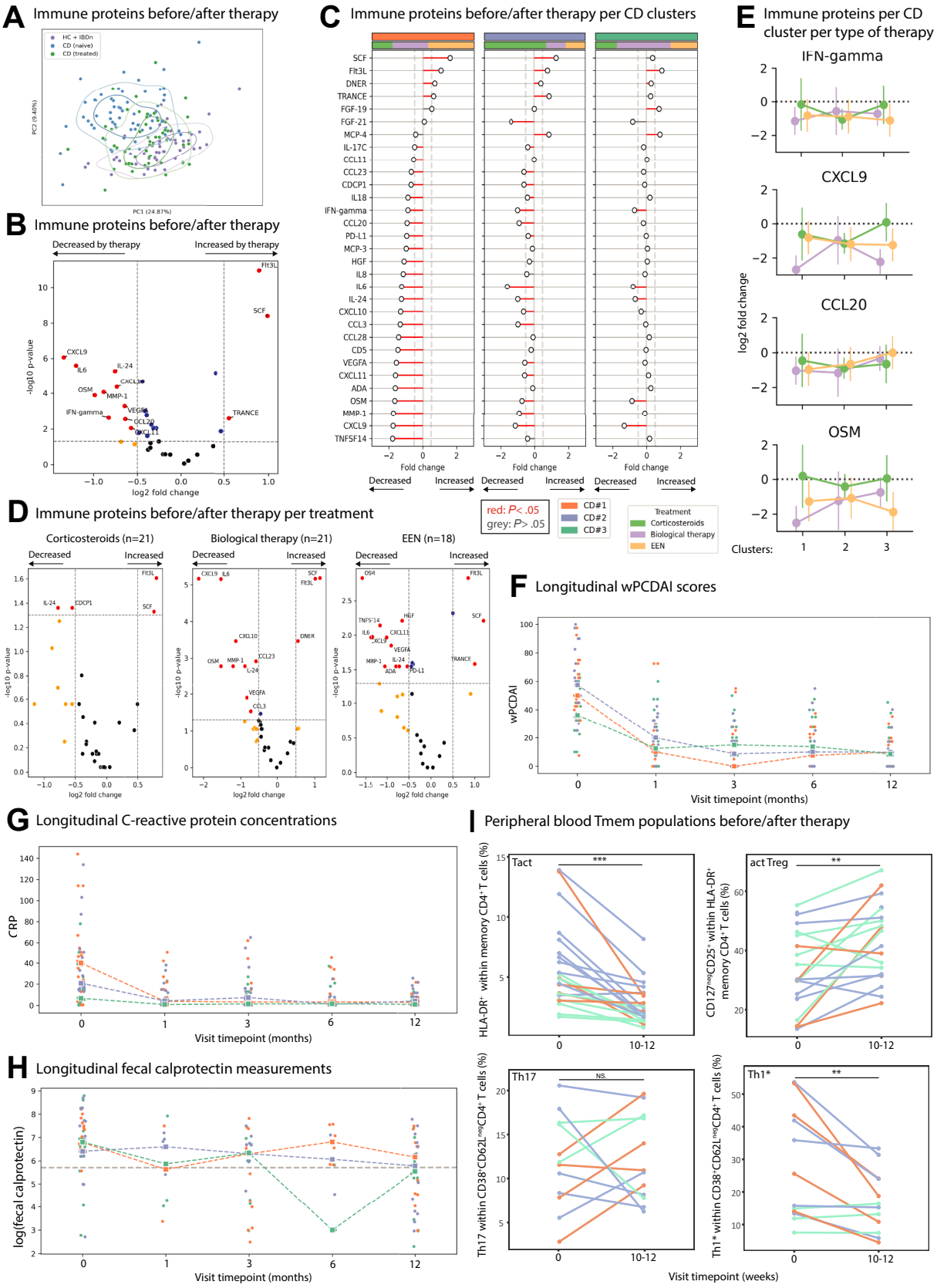

Fig. 6. CD clusters show differential responses to induction therapy but similar disease courses. A: Principal component analysis of all plasma proteins at t = 0 and t = 10–12 weeks (treated). B: Volcano plot of the 36 differential proteins at t = 10–12 weeks vs. t = 0. C: Fold changes in differential proteins in three CD clusters at t = 10–12 weeks vs. t = 0. D: Volcano plot of differential proteins at t = 10–12 weeks vs. t = 0 stratified by therapy. E: Fold changes in differential proteins at t = 10–12 weeks vs. t = 0 stratified by therapy. F-H: Longitudinal analysis of (F) wPCDAI score, (G) CRP, and (H) log fecal calprotectin per cluster. Dashed line indicates 300 mg/L fecal calprotectin. I: Peripheral blood Tmem frequencies at t = 0 and t = 10–12 weeks; *: $P < 0.05$, **: $P < 0.01$, ***: $P < 0.001$; paired Student *t* tests.

patients exhibited elevation of an Th17-related network (IL-17C, IL-17A, MMP10, CCL20, FGF-21, FGF-23; Fig. 4**A**). There were no clinicopathological features that distinguished these 5 patients from the rest of the CD#3 patients.

CD#1 and CD#2 both have an increased inflammatory ex-Th17/IFN-γ signature in blood and tissue but different abundances of proteins previously associated with poorer disease outcome

CD#1 and CD#2 had comparable clinicopathological parameters at diagnosis and high IFN-γ (Fig. 4**C,** Fig. S6**A**). CD#1 had significantly higher concentrations of the IFN-γ-induced proteins PD-L1, CXCL10 and CXCL11 vs. CD#2. TNFSF14, CCL28, and ADA were the top significantly increased proteins in CD#1 vs. CD#2 (Fig. 4**B**). TNFSF14, produced by neutrophils and T cells, enhances lymphocyte and neutrophil activation.[27,28] CCL28 drives homing of T and B cells and eosinophils.[29] ADA degrades adenosine, thereby enhancing inflammation.[30] Growth factors (VEGFA, HGF) and monocyte and neutrophil chemoattractants (MCP-3, MCP-4, IL-8) were also increased in CD#1 vs. CD#2 (Fig. 4**B**). Both TNFSF14 and HGF have been recently associated with poorer prognosis in moderate-to-severe CD.[22]

Frequencies of circulating Tmem significantly differed between CD clusters (Fig. 4**D**). CD#3 (lower inflammatory proteins) had lower frequencies of Tact than CD#2 and higher frequencies of actTreg than CD#1. Tact and actTreg frequencies were similar in CD#1 and CD#2. In line with this, CD#1 and CD#2 both had increased frequencies of Th1* cells in gut-homing $CD38^{+}CD62L^{neg}$ Tmem vs. CD#3. Other Tmem did not differ between CD clusters.

Histological disease severity (modified or activity GHAS) in ileum or colon did not differ between clusters, though fewer granulomata were detected in CD#3 biopsies (Fig. 4**E,** Table S5). Interestingly, ileal (but not colonic) CD#2 biopsies had more IL-1β-positive cells/mm^2 than CD#1 biopsies, although there was large heterogeneity between patients (Fig. 4**F**). Infiltrating neutrophils and IL-17A-secreting Th were similar between clusters (Fig. S6**B-C**). Intestinal mRNA expression analysis of Th1-related genes corroborated the differences in plasma immune profiles: *CXCL9, CXCL10, CXCL11* and *PD-L1* were increased in CD#1 and CD#2 ileal biopsies vs. CD#3, with no differences between CD#1 and CD#2; these differences were less evident in the colon (Fig. 4**G, S6D**).

Overall, the 36 plasma proteins discriminate three clusters in CD; two clusters have clinically more severe disease, increased frequencies of Tact and gut homing Th1* Tmem, and reduced frequencies of actTreg.

Clusters of protein concentrations in UC patients normalize in response to therapy, with earlier introduction of immunomodulators in more severe UC#2 than UC#1

Next, we assessed how baseline plasma immune profiles changed after induction therapy and determined whether the baseline clusters relate to disease course and therapeutic response in UC. No differences in plasma immune protein modulation were observed between the 14 patients (70 %) who received 5-aminosalicylates (5-ASA) and 6 (30 %) that received corticosteroids (Table S3). Overall, 10–12 weeks' induction therapy restored plasma immune profiles closer to the HC pattern (Fig. 5**A**). Induction therapy significantly decreased plasma IL-17A and FGF-21 and increased Ftl3L and TRANCE (Fig. 5**B**). Moreover, 12/36 differentially abundant proteins significantly changed in UC#1 and UC#2 after induction therapy (Fig. 5**C**). Counterintuitively, among UC#1, who had less severe disease and mostly received 5-ASA, induction therapy increased 10 plasma proteins, including inflammatory IFN-γ-induced CXCL10 and CXCL11, as well as ADA, HGF, and TNFSF14; this may be confounded by the small paired sample size (Fig.S7**A**). As expected, induction therapy slightly decreased IL-17A (non-significantly) and significantly reduced FGF-21 in UC#1. In addition, in UC#2, who were more severely affected and received 5-ASA or corticosteroids, induction therapy decreased IL-17A and FGF-21. Induction therapy only increased Flt3L in UC#2. Despite these changes in a small number of plasma proteins, peripheral blood Tmem did not differ between t = 10–12 weeks and diagnosis (Fig.S7**B**), in line with the absence of strong alterations in circulating Tmem in therapy-naïve UC vs. HC (Fig. 1**D**).

Induction therapy increased Flt3L and decreased FGF-21, regardless of whether patients received 5-ASA or corticosteroids (Fig. 5**D**). Longitudinal analysis revealed an effective reduction in the clinical severity of disease after induction and stability over the first year in both UC#1 and UC#2 (Fig. 5**E,** Table S6**)**. In contrast, fecal calprotectin was consistently higher in UC#2 than UC#1 up to 1 year. CRP remained low in all UC patients **(**Fig. 5**E)**. Despite the reduced plasma IL-17A and clinicopathological severity in UC#1 and UC#2, most patients (90 %) only had a "small" clinical response and only 55 % reached full clinical remission after induction therapy (56 % UC#1 vs. 55 % UC#2; Table S6). However, pretreatment stratification based on inflammatory immune protein profiles was more significantly related to clinical disease course over the longer term. Specifically, UC#2, with higher plasma immune profiles, required immunomodulation earlier than UC#1 (Fig. 5**F**). In agreement, a higher proportion of UC#2 required anti-TNFα within the first year than UC#1 (40 % vs. 11 %), although this difference was not statistically significant (Table S6**,** Fig.S8**A**). Overall, 10–12 weeks' induction therapy partially restored inflammatory plasma immune profiles in UC. Stratification based on inflammatory plasma immune proteins at diagnosis identifies patients who require earlier treatment escalation.

Clusters of CD patients show differential responses to therapy but a similar disease course

Overall, in CD, 10–12 weeks' induction therapy restored plasma immune protein profiles almost to the HC profile (Fig. 6**A**). Induction therapy was exclusive enteral nutrition (EEN) in 18 (29 %) patients, corticosteroids in 21 (34 %), and biologics in 21 (34 %; Table S3). One patient who received antibiotics and one patient who received 5-ASA were excluded. Treatment had more substantial effects on plasma protein concentrations in CD than UC. In CD, induction significantly reduced 10 inflammatory proteins (CXCL9, IL-6, IL-24, OSM, CXCL10, MMP-1, VEGFA, IFN-γ, CCL20, CXCL11) and significantly increased Flt3L, SCF, and TRANCE (Fig. 6**B**); these proteins included three of the five proteins that were highest at diagnosis in CD vs. HC (CXCL9, IL-6, OSM). Clear differences in response to therapy were detected between clusters: more plasma proteins (24 down-, 5 upregulated) were modulated with greater fold changes in CD#1, the cluster with higher inflammatory protein concentrations at diagnosis (Fig. 6**C**); CD#2 (intermediate pretreatment profiles) exhibited intermediate modulation (14 down-, 4 upregulated) and CD#3 (lowest pretreatment profiles, least severe clinical disease) exhibited fewer changes (5 down-, 3 upregulated; Fig. 6**C**). IFN-γ, IL-6, IL-24, OSM, and CXCL9 were consistently lower in all three clusters and Flt3L was consistently higher, suggesting correction of the inflammatory profile by treatment.

As the treatments varied among clusters, we investigated the effect of each therapy on plasma protein concentrations (Fig. 6**D**). Corticosteroids significantly increased Flt3L and SCF and reduced IL-24 and CDCP1. Biological therapy increased SCF, Flt3L, and DNER and reduced CXCL9, OSM, IL-6, MMP-1, CXCL10, IL-24, VEGFA, CCL3, and CCL23. EEN increased Flt3L, SCF, and TRANCE and reduced OSM, IL-6, CXCL9, TNFSF14, MMP-1, CXCL11, VEGFA, ADA, IL-24, HGF, and PD-L1; an almost complete overlap with the proteins altered by biological therapy. The fold changes per protein for each therapy per patient cluster (Fig. 6**E**) revealed high fold changes for IFN-γ and CCL20 in all clusters irrespective of therapy. However, CXCL9 was less reduced by biological therapy in CD#2 than the other clusters. OSM was less reduced by corticosteroids in CD#1 and CD#3. Overall, biological therapy (anti-TNFα) and EEN significantly reduced plasma inflammatory protein concentrations; anti-TNFα had the strongest quantitative effect and corticosteroids had a less pronounced effect.

Clinically, CD#1 and CD#2 achieved larger decreases in disease

score activity ("Moderate response"; Table S7) than CD#3. At t = 10–12 weeks, the remission rates were not significantly different between clusters (Table S7). The smaller change in clinical disease in CD#3 is most likely explained by the lower clinical disease score at diagnosis. Clinical remission was reached after induction therapy by only approximately half of CD patients. Longitudinal analysis revealed effective reductions in clinical disease activity scores (Fig. 6**F**), fecal calprotectin, and CRP (Fig. 6**G-H)** after 10–12 weeks' therapy in all three clusters; no differences in disease outcomes or clinical disease course were detected between clusters (Table S7**,** Fig.S8**B**).

In agreement with the reductions in the plasma immune profiles, the frequencies of circulating Tmem dramatically changed after induction therapy in CD. Inflammatory Tact and gut-homing Th1* were increased at diagnosis and strongly decreased after induction (Fig. 6**I**). Conversely, induction therapy increased frequencies of actTregs (Fig. 6**I**). Although the small sample size per cluster limits this analysis, CD#3 (lowest inflammatory profile at diagnosis) exhibited fewer changes in Tmem frequencies vs. CD#1 and CD#2. These data demonstrate that induction therapy effectively reduced inflammatory protein profiles and concomitant inflammatory Tmem frequencies in all three CD clusters.

Discussion

In this study, we demonstrate, in a therapy-naïve pediatric IBD cohort, that plasma immune protein profiles discriminate subgroups of CD and UC patients with different disease immunotypes. These immunotypes relate to circulating Tmem responses, clinical parameters, and intestinal disease and thus allow identification of the networks of cells and proteins driving immunopathogenesis in IBD. Therapeutic intervention normalizes immune protein profiles, reflecting the effects of therapy. Moreover, pretreatment stratification based on immune profiles identified UC patients who required earlier initiation of immunomodulators.

Plasma profiling identified two different clusters of UC patients at diagnosis. UC#2 had a greater extent of disease and severity of histological disease, with more severe infiltration of Th17 and neutrophils in lesional biopsies. Crucially, UC#2 required earlier initiation of thiopurine than UC#1. Greater disease extent and more severe clinicopathological features are prognostic,[31] but are heterogeneous and would not have discriminated all patients in UC#2. Thus, plasma proteomics represents a more sensitive technique to discriminate UC patients who will develop different disease courses and enable tailored treatment strategies.

UC#1 and UC#2 share a core signature of increased IL-17A, IL-8, CCL11, and MMP-10 vs. HC. High plasma IL-17A and increased abundance of IL-17A-producing cells in lesional biopsies are strongly associated with UC.[3] IL-17A drives recruitment of tissue damaging neutrophils by inducing IL-8.[32] However, IL-17A-secreting Th17 also promote barrier integrity and coordinate tissue protective responses.[24] CCL11, produced by macrophages and epithelial cells, selectively drives eosinophil recruitment and is increased in serum in UC.[33] MMP-10 is selectively increased in plasma in UC but not CD. MMP-10 is produced by macrophages and accumulates at healing ulcer edges in UC, possibly having a protective function.[34] Compared to UC#1, UC#2 had increased plasma IL-17A and MMP-10 and selective accumulation of CCL20 (which recruits CCR6-expressing Th17 to lamina propria), and IL-17C (which mediates neutrophil attraction and antimicrobial peptide production), thereby extending the core Th17/neutrophil-related signature. Additionally, UC#2 had higher plasma OSM, an inflammatory IL-6 family member; high pre-treatment OSM has been associated with anti-TNFα resistance and may have predictive value for a poor prognosis in CD and UC.[21,22,35,36] Crucially, selective accumulation of the IFN-γ-induced chemokines CXCL9, CXCL10, CXCL11, and CDCP-1 indicates that the UC#2 immunotype has Th1-related features that are absent in UC#1, in agreement with the significant correlation between histological disease activity and plasma IFN-γ (Fig. S4**B**) and increased intestinal *CXCL9* mRNA (Fig. 2**B**). This Th1-related response appears intestinally compartmentalized as circulating gut-homing Tmem did not differ between UC#1 or UC#2. In agreement, high-resolution single-cell analyses of UC lamina propria revealed increased ratios of IL-17A-IFN-γ-double-producing T cells in a subgroup of adult UC, suggesting intestinal ex-Th17 adopt a Th1-like profile in these patients.[37] The combined Th1/Th17-related immunotype in UC#2 could indicate a distinct immunopathogenesis leading to increased uncontrolled mucosal inflammation, greater disease extent, and more severe disease.

Plasma immune profiling identified three clusters of CD patients at diagnosis. CD#1 and CD#2 had higher concentrations of most inflammatory plasma proteins (particularly the IFN-γ pathway), increased frequencies of circulating IFN-γ-related HLADR$^+$ and gut-homing Th1* Tmem, and increased expression of IFN-γ-related mRNA in lesional biopsies vs. CD#3. Accordingly, CD#3 had less severe clinicopathological parameters than CD#1 and CD#2. Thus, immune profiling could avoid overtreatment of milder CD (CD#3) and enable initiation of more intensive induction treatment in more severe CD (CD#1, CD#2). The strong blood and tissue IFN-γ signature combined with increased circulating gut-homing Th1* Tmem implies that ex-Th17 drive disease in CD#2 and CD#1. Th1* are strong IFN-γ producers, pathogenic in inflammatory autoimmune disorders such as juvenile idiopathic arthritis, and have been identified in inflamed CD tissues[10]. Th1* pathogenicity may partly be related to expression of MDR-1 (or P-glycoprotein/ABCB1), a membrane efflux pump that binds glucocorticoids leading to resistance to corticosteroid therapy.[38,39]

Although exhibiting a similar IFN-γ-related signature, CD#1 and CD#2 have distinct plasma immune profiles with four notable differences. CD#1 has significantly higher plasma TNFSF14 (or LIGHT), which can enhance phagocyte bactericidal activity and lymphocyte proliferation, and higher HGF, which has a range of functions including angiogenesis and tissue regeneration.[27,28,40] In our previous study, high pre-treatment serum TNFSF14 and HGF were associated with poorer prognosis at 52 weeks in moderate-to-severe pediatric CD in the first-line arm.[22] In addition, CD#1 had higher plasma ADA than CD#2. Total ADA, an enzyme important for immune cell maturation, and its isoenzyme ADA2 were increased in the serum of CD patients with active disease vs. remission.[41] Finally, CD#1 had high plasma CCL28, a chemokine produced by epithelial cells that recruits CCR3- and CCR10-expressing T and B cells and eosinophils and has antimicrobial activity. Interestingly, inflammatory mediators, such as bacterial flagellin, IL-1, and the short chain fatty acid butyrate, elicit CCL28 production.[42] Together, these data argue that CD#1 may have a worse disease course than CD#2; a larger cohort with longer follow-up is required to assess this hypothesis.

In general, the plasma immune protein concentrations related to intestinal immune responses in lesional tissues and captured the extent of disease. However, plasma immune profiles were only associated with circulating gut-homing Tmem frequencies in CD. In UC, plasma immune protein profiles only relate to a small decrease in gut-homing Th2 vs. HC, which could indicate depletion from peripheral blood as a result of increased recruitment.[43] However, except for detection of eosinophil-recruiting chemokines, type-2 related intestinal inflammation or Th2-related plasma cytokines IL-13 and IL-5 were not different between UC and HC in contrast[6,7] and agreement[44] with previous studies. Some plasma cytokine concentrations were associated with disease location. In particular, IL-17A was directly associated with colonic involvement in CD. Intriguingly, high plasma IL-17A in CD is strongly associated with severe histological disease, indicating severe CD involves a stronger Th17-related response.

Plasma immune profiles partially restored to HC patterns after 10–12 weeks' induction therapy. However, seven CD patients maintained high concentrations of inflammatory proteins at week 10–12 (Fig. S9**A**). These patients had more severe clinicopathological parameters, indicative of remnant inflammation, but equivalent disease outcomes at one year (Fig.S9**B**, Table S8). This inception cohort received a variety of

different treatments; thus, we cannot assess which treatment strategy was most efficient for each cluster.

Although we anticipate that genetic susceptibility may play a role in the heterogeneity of the immune response in the identified patient clusters, we have not yet assessed IBD-associated polymorphisms in this cohort. It would be of particular interest to assess the HLA genes and the proinflammatory Th17-associated loci in our cohort, as they have been associated with increased IBD susceptibility and could relate to our results.[45,46]

Overall, immune plasma protein profiling is a powerful tool that discriminates individual patient immunotypes at diagnosis with high sensitivity. These data warrant future immune protein profiling studies to design tailored therapies and determine treatment success in randomized controlled trials.

Materials & methods

Patient selection

We enrolled children with newly diagnosed IBD and controls at the Erasmus Medical Center, Rotterdam, The Netherlands. IBD was diagnosed according to the revised Porto criteria[47] and classified as CD, UC, or IBD unclassified (IBD-U). IBD-U ($n = 3$) was grouped with UC. Twenty-two CD patients were selected from the TISKIDS RCT[48] (European Clinical Trial Register, EudraCT number 2014-005702-37). All other patients were selected from the PIBD-SETQuality inception cohort[49]. Participants with intestinal complaints and clinical suspicion of IBD but negative for IBD diagnosis after endoscopy were included as IBDneg controls. Blood from age-matched HC was collected from patients visiting the pediatric orthopedic department. Permission for the TISKIDS RCT and PIBD-SETQuality cohort was provided by the institutional ethical review board (MEC-2015-080 and MEC-2016-321). Informed consent was obtained from all patients and parents according to Dutch regulations.

Clinical data collection

Clinical data was collected at diagnosis and scheduled follow-ups at 10/12 weeks, 6 months, and 1 year after diagnosis (for details see supplemental methods). Intestinal biopsies were taken via endoscopy at diagnosis from macroscopically non-affected and macroscopically affected ileum and colon; paired adjacent biopsies were collected for histological analysis (for histology and histological scoring see supplemental methods) and RNA sequencing (see supplemental methods). After diagnosis, patients in the PIBD-SETQuality cohort started standard induction treatment alongside maintenance treatment as per the physician's discretion. Patients in TISKIDS received induction therapy of either five infusions of infliximab (biosimilar Inflectra®) in the first-line arm or EEN or corticosteroids in the conventional arm. All patients received azathioprine maintenance therapy. The primary outcomes were normal CRP remission at 10–12 weeks and sustained steroid-free remission (SSFR) at 1 year; see Table S1 for secondary outcomes and definitions/criteria.

Proximity extension assay

Plasma was collected from fresh whole blood EDTA tubes after centrifugation (321 x g, 10 min, room temperature), stored at −80 °C, and assessed using the 92 Inflammation Panel (Olink®, Sweden) assay. Concentrations are expressed as normalized protein expression (NPX; log2, arbitrary unit) after normalization of qPCR values. See supplemental methods for sample preparation, missing values and quality control.

Statistical analysis

For therapy-naïve sample analysis, Student *t* tests were performed per protein across pairs of patient disease groups and corrected for multiple testing using the Benjamini-Hochberg procedure, resulting in 36 differentially abundant proteins that differentiate IBD versus non-IBD. To discriminate UC and CD clusters, heatmaps of the z-scores of the NPX values were generated for the 36 differentially abundant proteins. To calculate z-scores, we subtracted CD and UC NPX-values per protein from the mean of HC + IBDneg samples and then divided by the standard deviation; a value around zero can be interpreted as a healthy average. Hierarchical clustering was performed using the Ward criterion on the z-scores of the 36 differentially abundant proteins. Changes in protein profiles were compared between three CD therapy groups (EEN, corticosteroids, anti-TNFα) and two UC therapy groups (5-ASA, corticosteroids). A mixed effect model was fitted on the protein concentrations before and after therapy, with treatment and time point as fixed effects and patients as random effects. After fitting, the differences in the coefficients of each treatment between time-points were used for statistical testing. Limma was used for partial pooling of coefficient standard errors across proteins to improve inference. Analyses were performed with Python version 3.9.6 (scipy 1.10.1, scikit-learn 1.2.2, statsmodels 0.14.0), R version 4.2.3 (limma 3.54.0), or SPSS version 26.0 (IBM Corporation, Armonk, NY, USA). For additional analyses see supplemental methods.

Funding

This work was supported by PIBD-SETQuality study WP9 supported by the European Union's Horizon 2020 Research and Innovation Program (grant agreement number 668023); stichting Dalijn and the collaborative TIMID project [LSHM18057-SGF] financed by the PPP allowance made available by Top Sector Life Sciences & Health to the Samenwerkende Gezondheidsfondsen [SGF] to stimulate public–private partnerships and co-financing by health foundations that are part of the SGF. The funders had no role in study design, data collection, statistical analysis, interpretation, or writing.

Author contributions

JNS, LdR, JCE, FMR, and NMC contributed to study concept, design, and funding. JNS and LdR supervised the study. MAA, MMEJ, RCWK, PK, DHHVH, BT, YSO, LAVB, and BBF contributed to patient recruitment, clinical data registration, experimental immunological analyses, and clinical data interpretation. SN and MD performed histological disease activity scoring. MAS, GVB, and BC performed RNA analysis. AM and MJTR supervised/contributed to statistical and bioinformatics analysis. MH, MC, RCWK, and JNS performed data analyses, had full access to study data, and take responsibility for data integrity. MH, MC, RCWK, and JNS drafted the manuscript. All authors contributed to critical revision of the manuscript, provided important intellectual content, and approved the final version of the manuscript.

Disclosures

FMR, NMC, JCE and LdR are involved in industry-sponsored studies/ investigator-initiated studies/ consultancy or received research support from AbbVie, BIOGEN, BMS, CAPE (ABBVIE), CELGENE, Centocor, Danone, Eli Lilly, Johnson & Johnson, MeadJohnson, Medtronic, MSD, MSD France, Nestlé Health Science, Nestlé Nutrition Institute, Pfizer, TAKEDA, SAC:DEVELOP (Johnson & Johnson). All other authors declare no conflict of interest.

Conference presentations

UEGweek 2021, virtual; UEGweek 2022; Joint Belgium-Dutch society for Immunology 2023.

CRediT authorship contribution statement

Maud Heredia: Writing – review & editing, Writing – original draft, Visualization, Investigation, Formal analysis, Data curation. **Mohammed Charrout:** Writing – review & editing, Writing – original draft, Visualization, Investigation, Formal analysis, Data curation. **Renz C.W. Klomberg:** Writing – review & editing, Writing – original draft, Investigation, Formal analysis, Data curation. **Martine A. Aardoom:** Writing – review & editing, Software, Project administration, Data curation. **Maria M.E. Jongsma:** Writing – review & editing, Methodology, Investigation. **Polychronis Kemos:** Software, Resources, Data curation. **Danielle H. Hulleman-van Haaften:** Investigation. **Bastiaan Tuk:** Investigation. **Lisette A. van Berkel:** Investigation. **Brenda Bley Folly:** Project administration, Methodology, Investigation. **Beatriz Calado:** Visualization, Formal analysis, Data curation. **Sandrine Nugteren:** Writing – review & editing, Investigation. **Ytje Simons-Oosterhuis:** Investigation. **Michail Doukas:** Investigation. **Mathijs A. Sanders:** Supervision, Formal analysis, Data curation. **Gregory van Beek:** Investigation, Data curation. **Frank M. Ruemmele:** Writing – review & editing, Project administration, Funding acquisition, Conceptualization. **Nicholas M. Croft:** Writing – review & editing, Supervision, Funding acquisition, Conceptualization. **Ahmed Mahfouz:** Supervision. **Marcel J.T. Reinders:** Writing – review & editing, Supervision. **Johanna C. Escher:** Writing – review & editing, Supervision, Project administration, Investigation, Funding acquisition. **Lissy de Ridder:** Writing – review & editing, Supervision, Project administration, Investigation, Funding acquisition. **Janneke N. Samsom:** Writing – review & editing, Writing – original draft, Supervision, Resources, Project administration, Methodology, Investigation, Funding acquisition, Conceptualization.

Declaration of Competing Interest

The authors declare that they have no known competing financial interests or personal relationships that could have appeared to influence the work reported in this paper.

Data availability

Data, analytic methods, and study materials will be made available to other researchers upon acceptance (repository URL: https://doi.org/10.34894/4DOZVN).

Acknowledgements

The authors thank Dr. Lea Costes and Dr. Irma Tindemans for contributing to study initiation and the PIBD-SETQuality consortium for valuable discussions. We thank A. Devlin from Science Editing Experts for editorial assistance (funded by internal resources).

Appendix A. Supplementary data

Supplementary data to this article can be found online at https://doi.org/10.1016/j.mucimm.2024.09.004.

References

1. Uhlig HH, Powrie F. Translating Immunology into Therapeutic Concepts for Inflammatory Bowel Disease. *Annu Rev Immunol*. 2018;36:755–781. https://doi.org/10.1146/annurev-immunol-042617-053055.
2. Tindemans I, Joosse ME, Samsom JN. Dissecting the Heterogeneity in T-Cell Mediated Inflammation in IBD. *Cells*. 2020;9. https://doi.org/10.3390/cells9010110.
3. Fujino S, et al. Increased expression of interleukin 17 in inflammatory bowel disease. *Gut*. 2003;52:65–70. https://doi.org/10.1136/gut.52.1.65.
4. Verdier J, Begue B, Cerf-Bensussan N, Ruemmele FM. Compartmentalized expression of Th1 and Th17 cytokines in pediatric inflammatory bowel diseases. *Inflamm Bowel Dis*. 2012;18:1260–1266. https://doi.org/10.1002/ibd.21905.
5. Reimund JM, et al. Increased production of tumour necrosis factor-alpha interleukin-1 beta, and interleukin-6 by morphologically normal intestinal biopsies from patients with Crohn's disease. *Gut*. 1996;39:684–689. https://doi.org/10.1136/gut.39.5.684.
6. Fuss IJ, et al. Disparate CD4+ lamina propria (LP) lymphokine secretion profiles in inflammatory bowel disease. Crohn's disease LP cells manifest increased secretion of IFN-gamma, whereas ulcerative colitis LP cells manifest increased secretion of IL-5. *J Immunol*. 1996;157:1261–1270. https://doi.org/10.4049/jimmunol.157.3.1261.
7. Li J, et al. Profiles of Lamina Propria T Helper Cell Subsets Discriminate Between Ulcerative Colitis and Crohn's Disease. *Inflamm Bowel Dis*. 2016;22:1779–1792. https://doi.org/10.1097/mib.0000000000000811.
8. Paroni M, et al. An Intestinal Th17 Subset is Associated with Inflammation in Crohn's Disease and Activated by Adherent-invasive Escherichia coli. *J Crohns Colitis*. 2023;17:1988–2001. https://doi.org/10.1093/ecco-jcc/jjad119.
9. Bsat M, et al. Differential Pathogenic Th17 Profile in Mesenteric Lymph Nodes of Crohn's Disease and Ulcerative Colitis Patients. *Front Immunol*. 2019;10:1177. https://doi.org/10.3389/fimmu.2019.01177.
10. Stadhouders R, Lubberts E, Hendriks RW. A cellular and molecular view of T helper 17 cell plasticity in autoimmunity. *J Autoimmun*. 2018;87:1–15. https://doi.org/10.1016/j.jaut.2017.12.007.
11. Steimle V, Siegrist CA, Mottet A, Lisowska-Grospierre B, Mach B. Regulation of MHC class II expression by interferon-gamma mediated by the transactivator gene CIITA. *Science*. 1994;265:106–109. https://doi.org/10.1126/science.8016643.
12. Nathan CF, Murray HW, Wiebe ME, Rubin BY. Identification of interferon-gamma as the lymphokine that activates human macrophage oxidative metabolism and antimicrobial activity. *J Exp Med*. 1983;158:670–689. https://doi.org/10.1084/jem.158.3.670.
13. Brabec T, et al. IL-17-driven induction of Paneth cell antimicrobial functions protects the host from microbiota dysbiosis and inflammation in the ileum. *Mucosal Immunol*. 2023;16:373–385. https://doi.org/10.1016/j.mucimm.2023.01.005.
14. Brackman LC, et al. IL-17 receptor A functions to help maintain barrier integrity and limit activation of immunopathogenic response to H. pylori infection. *Infect Immun*. 2024;92:e0029223.
15. Flannigan KL, et al. IL-17A-mediated neutrophil recruitment limits expansion of segmented filamentous bacteria. *Mucosal Immunol*. 2017;10:673–684. https://doi.org/10.1038/mi.2016.80.
16. Schroepf S, et al. Strong overexpression of CXCR3 axis components in childhood inflammatory bowel disease. *Inflamm Bowel Dis*. 2010;16:1882–1890. https://doi.org/10.1002/ibd.21312.
17. Kaser A, et al. Increased Expression of CCL20 in Human Inflammatory Bowel Disease. *J Clin Immunol*. 2004;24:74–85. https://doi.org/10.1023/b:joci.0000018066.46279.6b.
18. Moraes L, et al. Systemic Inflammatory Protein Profiles Distinguish Irritable Bowel Syndrome (IBS) and Ulcerative Colitis, Irrespective of Inflammation or IBS-Like Symptoms. *Inflamm Bowel Dis*. 2020;26:874–884. https://doi.org/10.1093/ibd/izz322.
19. Ungaro RC, et al. Machine learning identifies novel blood protein predictors of penetrating and stricturing complications in newly diagnosed paediatric Crohn's disease. *Aliment Pharmacol Ther*. 2021;53:281–290. https://doi.org/10.1111/apt.16136.
20. Walshe M, et al. A role for CXCR3 ligands as biomarkers of post-operative Crohn's disease recurrence. *J Crohns Colitis*. 2021. https://doi.org/10.1093/ecco-jcc/jjab186.
21. Kalla R, et al. Serum proteomic profiling at diagnosis predicts clinical course, and need for intensification of treatment in inflammatory bowel disease. *J Crohns Colitis*. 2021;15:699–708. https://doi.org/10.1093/ecco-jcc/jjaa230.
22. Jongsma MME, et al. Serum immune profiling in pediatric Crohn's disease demonstrates stronger immune modulation with first-line infliximab than conventional therapy and pre-treatment profiles predict clinical response to both treatments. *J Crohns Colitis*. 2023. https://doi.org/10.1093/ecco-jcc/jjad049.
23. Joosse ME, et al. Frequencies of circulating regulatory TIGIT(+)CD38(+) effector T cells correlate with the course of inflammatory bowel disease. *Mucosal Immunol*. 2019;12:154–163. https://doi.org/10.1038/s41385-018-0078-4.
24. Omenetti S, et al. The Intestine Harbors Functionally Distinct Homeostatic Tissue-Resident and Inflammatory Th17 Cells. *Immunity*. 2019;51:77–89 e76. https://doi.org/10.1016/j.immuni.2019.05.004.
25. Veenbergen S, et al. IL-10 signaling in dendritic cells controls IL-1beta-mediated IFNgamma secretion by human CD4(+) T cells: relevance to inflammatory bowel disease. *Mucosal Immunol*. 2019;12:1201–1211. https://doi.org/10.1038/s41385-019-0194-9.
26. Friedrich M, et al. IL-1-driven stromal-neutrophil interactions define a subset of patients with inflammatory bowel disease that does not respond to therapies. *Nat Med*. 2021;27:1970–1981. https://doi.org/10.1038/s41591-021-01520-5.
27. Heo SK, et al. LIGHT enhances the bactericidal activity of human monocytes and neutrophils via HVEM. *J Leukoc Biol*. 2006;79:330–338. https://doi.org/10.1189/jlb.1104694.
28. Tamada K, et al. LIGHT, a TNF-like molecule, costimulates T cell proliferation and is required for dendritic cell-mediated allogeneic T cell response. *J Immunol*. 2000;164:4105–4110. https://doi.org/10.4049/jimmunol.164.8.4105.
29. Wang W, et al. Identification of a novel chemokine (CCL28), which binds CCR10 (GPR2). *J Biol Chem*. 2000;275:22313–22323. https://doi.org/10.1074/jbc.M001461200.
30. Antonioli L, et al. Inhibition of adenosine deaminase attenuates inflammation in experimental colitis. *J Pharmacol Exp Ther*. 2007;322:435–442. https://doi.org/10.1124/jpet.107.122762.
31. Orlanski-Meyer E, et al. Predicting Outcomes in Pediatric Ulcerative Colitis for Management Optimization: Systematic Review and Consensus Statements From the

Pediatric Inflammatory Bowel Disease-Ahead Program. *Gastroenterology*. 2021;160:378–402 e322. https://doi.org/10.1053/j.gastro.2020.07.066.
32. Laan M, et al. Neutrophil recruitment by human IL-17 via C-X-C chemokine release in the airways. *J Immunol*. 1999;162:2347–2352. https://doi.org/10.4049/jimmunol.162.4.2347.
33. Ahrens R, et al. Intestinal macrophage/epithelial cell-derived CCL11/eotaxin-1 mediates eosinophil recruitment and function in pediatric ulcerative colitis. *J Immunol*. 2008;181:7390–7399. https://doi.org/10.4049/jimmunol.181.10.7390.
34. Koller FL, et al. Lack of MMP10 exacerbates experimental colitis and promotes development of inflammation-associated colonic dysplasia. *Lab Invest*. 2012;92:1749–1759. https://doi.org/10.1038/labinvest.2012.141.
35. West NR, et al. Oncostatin M drives intestinal inflammation and predicts response to tumor necrosis factor-neutralizing therapy in patients with inflammatory bowel disease. *Nat Med*. 2017;23:579–589. https://doi.org/10.1038/nm.4307.
36. Verstockt S, et al. Oncostatin M Is a Biomarker of Diagnosis, Worse Disease Prognosis, and Therapeutic Nonresponse in Inflammatory Bowel Disease. *Inflamm Bowel Dis*. 2021;27:1564–1575. https://doi.org/10.1093/ibd/izab032.
37. Mitsialis V, et al. Single-Cell Analyses of Colon and Blood Reveal Distinct Immune Cell Signatures of Ulcerative Colitis and Crohn's Disease. *Gastroenterology*. 2020;159:591–608 e510. https://doi.org/10.1053/j.gastro.2020.04.074.
38. Ramesh R, et al. Pro-inflammatory human Th17 cells selectively express P-glycoprotein and are refractory to glucocorticoids. *J Exp Med*. 2014;211:89–104. https://doi.org/10.1084/jem.20130301.
39. Bourgeois S, Gruol DJ, Newby RF, Rajah FM. Expression of an mdr gene is associated with a new form of resistance to dexamethasone-induced apoptosis. *Mol Endocrinol*. 1993;7:840–851. https://doi.org/10.1210/mend.7.7.8105374.
40. Kato T. Biological roles of hepatocyte growth factor-Met signaling from genetically modified animals. *Biomed Rep*. 2017;7:495–503. https://doi.org/10.3892/br.2017.1001.
41. Maor I, Rainis T, Lanir A, Lavy A. Adenosine deaminase activity in patients with Crohn's disease: distinction between active and nonactive disease. *Eur J Gastroenterol Hepatol*. 2011;23:598–602. https://doi.org/10.1097/MEG.0b013e328346e205.
42. Ogawa H, Iimura M, Eckmann L, Kagnoff MF. Regulated production of the chemokine CCL28 in human colon epithelium. *Am J Physiol Gastrointest Liver Physiol*. 2004;287:G1062–G1069. https://doi.org/10.1152/ajpgi.00162.2004.
43. Rubin SJS, et al. Mass cytometry reveals systemic and local immune signatures that distinguish inflammatory bowel diseases. *Nat Commun*. 2019;10:2686. https://doi.org/10.1038/s41467-019-10387-7.
44. Biancheri P, et al. Absence of a role for interleukin-13 in inflammatory bowel disease. *Eur J Immunol*. 2014;44:370–385. https://doi.org/10.1002/eji.201343524.
45. Ashton JJ, Latham K, Beattie RM, Ennis S. Review article: the genetics of the human leucocyte antigen region in inflammatory bowel disease. *Aliment Pharmacol Ther*. 2019;50:885–900. https://doi.org/10.1111/apt.15485.
46. Medina TS, et al. The chromatin and single-cell transcriptional landscapes of CD4 T cells in inflammatory bowel disease link risk loci with a proinflammatory Th17 cell population. *Front Immunol*. 2023;14:1161901. https://doi.org/10.3389/fimmu.2023.1161901.
47. Levine A, et al. ESPGHAN revised porto criteria for the diagnosis of inflammatory bowel disease in children and adolescents. *J Pediatr Gastroenterol Nutr*. 2014;58:795–806. https://doi.org/10.1097/MPG.0000000000000239.
48. Jongsma MME, et al. First-line treatment with infliximab versus conventional treatment in children with newly diagnosed moderate-to-severe Crohn's disease: an open-label multicentre randomised controlled trial. *Gut*. 2022;71:34–42. https://doi.org/10.1136/gutjnl-2020-322339.
49. Aardoom MA, et al. International prospective observational study investigating the disease course and heterogeneity of paediatric-onset inflammatory bowel disease: the protocol of the PIBD-SETQuality inception cohort study. *BMJ Open*. 2020;10:e035538.